RSC Advances

ROYAL SOCIETY OF CHEMISTRY

www.rsc.org/advances

Synthesize nano-size (~20nm) $Li_4Ti_5O_{12}$ under low temperature as anode for high rate performance lithium ion battery

Chongling Cheng[a,c], Hongjiang Liu[b,c*], Xin Xue[b,c], Shaomei Cao[a,c],Hui Cao[d], Liyi Shi[abc*]

a .Nano-Science & Technology Research Center, Shanghai University, No.99 Shangda Road, Shanghai, 200444, P. R. China,. Fax: +86 21 66136038 Tel: +86-21 66136069;

b. college of science, Shanghai University,. No.99 Shangda Road, Shanghai, 200444, P. R. China,. Fax: +86 21 66136038 Tel: +86-21 66136069;

c Professional and Technical Service Platform for Designing and Manufacturing of Advanced Composite Materials,shanghai,200444, P.R.China.,

d. Shanghai Aerospace Power Technology Co. Ltd, P. R. China Shanghai, 201615, P.R.China.,

The corresponding author is Associate professor Hongjiang Liu and his address and other information is as following:

Associate professor Hongjiang Liu

E-mail: hjliushu@hotmail.com

Tel: +86-21 66136069 Fax: +86-21 66136038

abstract： In this paper, we developed a novel strategy to synthesize nano-size $Li_4Ti_5O_{12}$ (LTO) by hydrothermal and calcined under low temperature. X-ray diffraction and high resolution transmission electron microscopy measurements were performed to characterize the structures and morphologies of these samples. Highly crystallized and pure-phase $Li_4Ti_5O_{12}$ synthesized at low calcinations temperature about 500 ^oC was firstly reported. This nanocrystalline LTO was tested as the anode material for lithium ion batteries, and exhibited excellent reversible capacities of 166, 162, 155, 142 and 123 mA $h \cdot g^{-1}$ at current densities of 1 C, 2 C, 5 C,10 C and 20 C, respectively. It also demonstrated good capacity retentions and high coulombic efficiencies at all current rates. The excellent electrochemical performance makes our LTO to be a promising anode material for high energy/power density lithium ion batteries.

Key words: lithium ion battery; lithium titanate; nano-size; high rate performance

Recently, rechargeable lithium ion batteries (LIBs) have attracted more and more attention as one of the most potential candidates for electric vehicles (EVs), stationary power storage devices and portable power source for micro electric devices[1-5]. However, the cycle life and safety are the key obstructs that affecting it widely applied in this field[6]. Spinel $Li_4Ti_5O_{12}$ (LTO) is one of the most attractive negative electrode materials that may solve these problems[7, 8]. LTO displays excellent stability owing to its volume expansion/contraction (<1%) when lithium ion intercalation and deintercalation, compare to approximately 9% volume change if the carbon materials used as anodes in commercial LIBs[2]. Furthermore, LTO exhibits a high plateau voltage in the Li insertion potential at approximately 1.55 V (versus Li^+/Li) [9]. As the consequence, it does not form a solid electrolyte interface with high resistance[10]. However, $Li_4Ti_5O_{12}$ has some disadvantages, such as it has so low theoretical capacity of 175 mA $h \cdot g^{-1}$ and pretty low electronic conductivity (ca. 10^{-13} $S \cdot cm^{-1}$), thus it is not satisfied for such applications[2, 11, 12].

In order to solve these problems, several researches have been done such as reducing the particle size and coating conductive materials on the $Li_4Ti_5O_{12}$ surface, or doping some metal ions[9]. Coating conductive materials on the surface enhance the electrical contact in the electrode is one of the common methods. Carbon is the most inexpensive and widely used material for modifying $Li_4Ti_5O_{12}$, because of it could increase electrical conductivity[13-15]. The LTO particles doped with different metal ions has been widely studied, such as Ag^+, Ru^{2+}, Cr^{4+} and V^{5+}, to increase their intrinsic conductivity so as to obtain a satisfactory level of power density[16-22].Decreasing the

particle size was one of the most useful ways, which could shorter the diffusion path of electrons and lithium ions as well as enlarging the contact area between the electrode and electrolyte[23]. For instance, Liu et al. use F127 to prepare the $Li_4Ti_5O_{12}$ with average of 20 nm[23]. Xia et al. prepared a series of $Li_4Ti_5O_{12}$ particles with average grain sizes of around 50 nm.[9, 24] Sun et al. reported a micro-sized $Li_4Ti_5O_{12}$ material composed of nanoscale (~100 nm) primary particles[25]. In these reports, relatively high calcinations temperatures (>700 ^oC) and complex steps are required to obtain highly crystallized $Li_4Ti_5O_{12}$, which inevitably induces the growth of $Li_4Ti_5O_{12}$ particles and makes it hard for commercial production. So far, it remains a great challenge to develop a facile approach to synthesize nano-sized and highly crystallized $Li_4Ti_5O_{12}$ in low temperature.

Here we reported a novel strategy to synthesize highly crystallized $Li_4Ti_5O_{12}$ (~20 nm). To the best of our knowledge, this is the first report about the preparation of highly crystallized $Li_4Ti_5O_{12}$ with a small particle size of ~20 under low synthesis temperature (500 ^oC). The as-derived nanocrystalline $Li_4Ti_5O_{12}$ sample was tested as the anode material for lithium ion batteries, exhibiting a superior reversible capacity of 123 mA h g^{-1} at 20 C and good cycling performance even at high current densities.

Experimental

Preparation of nano-LTO

All the reagents were purchased from China National Medicines Corp., Ltd without any purification

The LTO nanoparticles was fabricated by hydrothermal method .Typically, ammonium hydroxide (12.5% v/v, AR) wasdripped into 200 ml $TiOSO_4$ (1 M, AR) solution with the aid of ultrasonication, until the pH of solution was about 6. Subsequently, the TiO_2 was collected by centrifuge and wash with deionized water for more than 3 times.

5.0 g TiO_2 (solid content 20%) and 0.5 g $LiOH \cdot H_2O$ (AR) was dispersed in 30 ml deionized water, and stirring for more than 30 min. Then the suspension was transferred into a 50 ml Teflon-lined stainless steel autoclave and kept at 180 ^oC for 24 h. The precipitate was separated by vacuum-filtered, washed with deionized water several times. In order to remove the excess water of the precursor, it was kept in vacuum desiccators at -40 ^oC for 24 h. Finally, the LTO persour was calcined at different temperature in atmosphere to obtain nanaosize-$Li_4Ti_5O_{12}$ materials.

Characterization

The thermal gravity and differential scanning calorimetry curve of $Li_4Ti_5O_{12}$ precursor was recorded on 2960 SDT from room temperature to 800 ^oC with a heating rate of 5 $^oC \cdot min^{-1}$ under air flow. The crystal structures of the powders were studied using an X-ray diffraction (XRD) system (18KW D/MAX2200V PC Rigaku) with CuKa radiation from 10 to 70°. High resolution transmission electron microscopy (HRTEM, JEOL-2010F) was used to characterize the morphologies of the powders.

The electrochemistry performances were measured with coin cells, in which lithium metal foil was used as the counter electrode. The electrolyte employed was

1M solution of $LiPF_6$ in ethylene carbonate and dimethyl carbonate (EC+DMC) (1:1 in volume). The active materials powder (80 wt%), acetylene black (Super P, supplied by Timcal Inc. 10 wt%) and polyvinylidene fluoride (PVDF) binder (10 wt%) were homogeneously mixed in N-Methyl pyrrolidinone (NMP) solvent with magnetic stirring. After stirring for 24 h, the slurry was coated uniformly on copper foil. Finally, the electrode was dried under vacuum at 120 ^{o}C for 8h. Cell assembly was carried out in an argon-filled glove box ([O_2] < 1 ppm, [H_2O] < 1 ppm). The coin cells were cycled under different current densities between cut off voltages from 2.5 to 1.0 V on CT2001A cell test instrument (LAND Electronic Co. Ltd) at 20 ^{o}C. And electrochemical impedance spectroscopy (EIS) was carried out in the frequency range from 100 kHz to 10 mHz with an electrochemical workstation (CHI660E).

Results and discussion

Fig.1 showed the TG-DSC curves of the precursor powders with a heating rate of 5 ^{o}C·min^{-1} from 25 ^{o}C to 800 ^{o}C in air atmosphere. The first step of weight loss, observing between room temperature and about 200 ^{o}C, was mainly due to the vaporization of absorbed water. It corresponded to an endothermic peak around 100 ^{o}C on the DSC curve. The weight loss in the second step (mainly at 500 ^{o}C) was attributed to the decomposition of Ti-OH and Li-OH bonds. When the temperature was above 400 ^{o}C, the thermogravimetry (TG) curve showed nearly constant weight, indicating that the reaction is complete. Therefore, it was necessary to sinter the precursor mixture above 400 ^{o}C to get the well crystallized LTO phase.

<figure 1>

Fig. 2 showed the XRD patterns of the $Li_4Ti_5O_{12}$ (LTO) precursor calcined at different temperatures. From 400 ^oC to 600 ^oC, the diffraction peaks became more sharply and well defined, indicating that the crystal intensity improved along with the increase of temperature. For the sample calcined at 500 ^oC, the diffraction peaks at 2θ= 18.4, 35.6, 37.1, 43.3, 47.4, 57.2, 62.8 and 66.1^o could be indexed to the cubic spinel LTO (JCPDS card no. 49-0207) with Fd-3m space group. In addition, a tiny reflections at 2θ= 45.2^o was detected, when the LTO precursor calcined at 600 ^oC. It suggested the existence of a trace of as impurities and proves the temperature was too high. Therefore, a pure-phase and highly crystallized LTO could be obtained at a relative low temperature of 500 ^oC. By using Scherer's formula based on the (111) peak, the grain sizes of $Li_4Ti_5O_{12}$ (500 ^oC) were estimated to be 17.5 nm, which was much smaller than that reported in other publications[26-28].

<figure 2>

The nano-LTO featured a uniform particle size distribution as revealed by the typical TEM images, which was showed in Fig. 3. The Fig. 3d indicated that the particle size of the prepared LTO-500 was 18 nm, which was consistent with the XRD result. And the dimension of LTO-400 was similar to the LTO-500, which was showed in figure 3b. However, its lattice fringes were not clear owing to its low crystal degree. In the contrast, the size of LTO-600 became almost 50 nm when the temperature increased to 600 ^oC, which was showed in Fig.3 e. The HRTEM image of LTO-600 surface was showed in Fig.3 f.

<figure 3>

It could find that the surface of LTO was melted and the lattice fringe was unordered, which meant the calcined temperature was high. This bad surface may have bad effect of the Li ion insertion/deinsertion and its contact with electrolyte. Fig. 3 d showed that the entire grain particle of $Li_4Ti_5O_{12}$ was highly crystallized and the further revealed that the crystalline region with clear lattice fringes had an inter-planar spacing of 0.48 nm, consistent with the (111) atomic planes of the spinel structure. These results proved that the diameter of the LTO was affected by the claimed temperature. The higher temperature was not only increasing the diameter of the grains, but also making it surface liquation. That bad surface structure may lead bad electrochemistry performance.

<figure 4>

To evaluate the cycle performance of the prepared samples, we measured the charge/discharge capacities of LTO-500 and LTO-600 at different current rates (1 C, 2 C, 5 C 10 C and 20 C). For each stage, the batteries were cycled for 50 times. The capacity of LTO-500 was 166, 162, 155, 142 and 123 $mAhg^{-1}$ at 1 C, 2 C, 5 C, 10 C and 20 C, and the capacity of LTO-600 was 163, 160, 148, 116 and 74 $mAhg^{-1}$ at 1 C, 2 C, 5 C, 10 C and 20 C, respectively. In a addition, the capacity of LTO-400 was 164, 150, 137, 112 and 56 $mAhg^{-1}$ at 1 C, 2 C, 5 C, 10 C and 20 C, respectively. The low capacity and bad rate performance of LTO-400 owe to its low crystal degree.

The capacity difference between the LTO-500 and LTO-400, LTO-600 became more pronounced with the increased current rate, respectively. As shown in Fig. 4, very stable cycle ability was observed for LTO-500 at each current rate. The capacity

loss was less than 0.1% per cycle at all measured current rates, indicating the high stability of the nano-LTO in repeated cycles. In addition, the coulombic efficiency of nano-LTO approaches 100% for each cycle .Although the capacities of LTO-600 at high current rates were lower than those of LTO-500, the capacities kept stable at all current rates owing to its high crystallization. The bad rate performance of the LTO-600 may owing to its larger particle size and melted surface, which also proved that little particle size and good surface could contribute the electrochemistry performance of LTO. However, the electrochemical performance of LTO-400 was become worse along with the increasing current rate. The reason why the capacity of LTO-400 was so poor owning to its lower crystal degree. In a word, the performance of LTO-500 was much higher than the other LTO electrodes[2, 29-31].

<figure 5>

The discharge curves of LTO electrode cycled under different current densities with the voltages limits of 1-2.5 V were showed in Fig. 5. Flat discharge plateaus at about 1.55V were observed, suggesting that the discharge plateau of the LTO-500 was better than LTO-600 and LTO-400, owing to its small size and better crystal degree.

<figure 6>

We then resorted to electrochemical impedance spectroscopy (EIS) measurements to understand their intrinsic origins for the improved high-rate performance of the LTO samples. Fig. 6 showed the electrochemical impedance spectroscopy of the LTO-500 and LTO-600 measured at a stable voltage of 1.55 V. The data were analyzed by using the equivalent circuit model. In this model, R_s represents the ohmic

resistance including total resistance of the electrolyte, separator, and electrical contacts. R_{ct} was the charge-transfer resistance and CPE was the constant phase-angle element involving double layer capacitance. Z_W (Warburg impedance) reflects the solid-state diffusion of Li^+ in the bulk of the active material.

Apparently, the R_{ct} of LTO-500 (119 Ω) was much smaller than that of LTO-600 (258 Ω). We further calculate the charge-transfer kinetic parameter i^0 (exchange current density) by the following equation ($i_0=RT/nFR_{ct}$) where R_{ct} was the gas constant, T was the absolute temperature, n was the number of electrons involved in the charge-transfer reaction, and F was the Faraday constant. The derived i_0 value of LTO-500 (0.2 $mA\cdot cm^2$), which was higher than that of LTO-600 (0.09 $mA\cdot cm^2$). The accelerated charge-transfer kinetics of the LTO-500 sample could be ascribed to the small size and larger electrode/electrolyte contact area.

Meanwhile, the nano grain size of LTO-500 dramatically shortens the diffusion length of lithium ions, thus significantly improving lithium storage kinetics in the bulk of the active material. According to the above analysis, the accelerated charge-transfer kinetics and lithium-storage kinetics contribute collectively to the promotion of rate performance for the LTO-500. Obviously, the samples calcined at 600 ^oC suffer from capacity fading. It was also increase the alternating-cureent impedance. This phenomenon was caused by the existence of impurities in the surface under high calcination temperature. This was because of the increase of calcination temperature could induce the grain growth, thus adversely affecting the charge/transfer and lithium storage kinetics.

Conclusions

To summarize, we design a novel approach to synthesize nanosize-$Li_4Ti_5O_{12}$ under low temperature. Pure-phase and highly crystallized $Li_4Ti_5O_{12}$ with a small particle size of ~20 nm was obtained at a relatively low calcination temperature of 500^oC. Owing to its small diameter, the LTO anode exhibited a high reversible capacity of 123 mA h·g^{-}1 at 20 C and excellent cycling performance even at high current densities. The intrinsic advantage of $Li_4Ti_5O_{12}$ combined with the high-rate performance makes our nano-LTO a promising anode material for the development of high energy density lithium batteries directed to the plug-in hybrid electric vehicles and electric vehicle markets.

Acknowledge

The authors thanks for the Mr. Pengfei Hu and Mr. Jianchao Peng for his help in HRTEM characterization and Professor Dayang Wang for discussion. This work was financially supported by Shanghai Municipal Science and Technology Commission (11160704000, 12nm0500100 and 13DZ2292100).And The research also supported Baoshan District Science and Technology Commission of Shanghai (no. bkw2013142).

Reference：

1. X. Lu, L. Zhao, X. He, R. Xiao, L. Gu, Y. S. Hu, H. Li, Z. Wang, X. Duan, L. Chen, J. Maier and Y. Ikuhara, *Adv Mater*, 2012, **24**, 3233-3238.

2. L. Zhao, Y. S. Hu, H. Li, Z. Wang and L. Chen, *Adv Mater*, 2011, **23**, 1385-1388.

3. X. Chen, C. Li, M. Gratzel, R. Kostecki and S. S. Mao, *Chemical Society reviews*, 2012, **41**, 7909-7937.

4. Y.-Q. Wang, L. Gu, Y.-G. Guo, H. Li, X.-Q. He, S. Tsukimoto, Y. Ikuhara and L.-J. Wan, *J. Am. Chem. Soc.*, 2012, **134**, 7874-7879.

5. N. Du, H. Zhang, X. Fan, J. Yu and D. Yang, *Journal of Alloys and Compounds*, 2012, **526**, 53-58.

6. A. Gohier, Barbara Laïk , K.-H. Kim, J.-L. Maurice, Jean-Pierre, Pereira-Ramos, C. S. Cojocaru and P. T. Van, *Adv. Mater.*, 2012, **24**, 2592-2597.

7. Guodong Du, Neeraj Sharma , Vanessa K. Peterson, Justin A. Kimpton , Dianzeng Jia and Zaiping Guo, *Adv. Funct. Mater.*, 2011, **21**, 3990-3997.

8. C. Cheng, J. Wang, H. Liu, D. Zhang and L. Shi, *Advanced Materials Research*, 2012, **557-559**, 1214-1217.

9. G.-N. Zhu, Y.-G. Wang and Y.-Y. Xia, *Energy Environ. Sci.*, 2012, **5**, 6652-6667.

10. X. Li, M. Qu and Z. Yu, *Solid State Ionics*, 2010, **181**, 635-639.

11. M. S. Song, A. Benayad, Y. M. Choi and K. S. Park, *Chem Commun (Camb)*, 2012, **48**, 516-518.

12. K. Amine, I. Belharouak, Z. Chen, T. Tran, H. Yumoto, N. Ota, S.-T. Myung and Y.-K. Sun, *adv. Mater.*, 2010, **22**, 3052-3057.

13. M.-L. Lee, Y.-H. Li, S.-C. Liao, J.-M. Chen, J.-W. Yeh and H. C. Shih, *Applied Surface Science*, 2012, **258**, 5938-5942.

14. B. Li, C. Han, Y.-B. He, C. Yang, H. Du, Q.-H. Yang and F. Kang, *Energy & Environmental Science*, 2012, **5**, 9595.

15. L. Shen, C. Yuan, H. Luo, X. Zhang, L. Chen and H. Li, *Journal of Materials Chemistry*, 2011, **21**, 14414-14416.

16. Huang S, Wen Z, Zhang J and Yang X, *Electrochem. Acta*, 2007, **52**, 3704-3708.

17. W. Wang, H. Wang, S. Wang, Y. Hu, Q. Tian and S. Jiao, *J. Power Sources*, 2013, **228**, 244-249.

18. V. Aravindan, W. Chuiling and S. Madhavi, *Journal of Materials Chemistry*, 2012, **22**, 16026.

19. W.-T. Kim, Y. U. Jeong, H. C. Choi, Y. J. Lee, Y. J. Kim and J. H. Song, *Journal of Power Sources*, 2013, **221**, 366-371.

20. S. Huang, Z. Wen, X. Zhu and Z. Gu, *Electrochemistry Communications*, 2004, **6**, 1093-1097.

21. J. Wang, H. Zhao, Q. Yang, T. Zhang and J. Wang, *Ionics*, 2012, **19**, 415-419.

22. R. Cai, S. Jiang, X. Yu, B. Zhao, H. Wang and Z. Shao, *J. Mater. Chem.*, 2012, **22**, 8013-8021.

23. Z. Liu, N. Zhang and K. Sun, *Journal of Materials Chemistry*, 2012, **22**, 11688.

24. L. Cheng, J. Yan, G. N. Zhu, J. Y. Luo, C. X. Wang and Y. Y. Xia, *Journal of Materials Chemistry*, 2010, **20**, 595-602.

25. H.-G. Jung, S.-T. Myung, C. S. Yoon, S.-B. Son, K. H. Oh, K. Amine, B. Scrosati and Y.-K. Sun, *Energy & Environmental Science*, 2011, **4**, 1345.

26. X. Guo, C. Wang, M. Chen, J. Wang and J. Zheng, *Journal of Power Sources*, 2012, **214**, 107-112.

27. H. Li , L. Shen, X. Zhang, J. Wang, P. Nie, Q. Che and B. Ding, *Journal of Power Sources*, 2013, **221**, 122-127.

28. Y. B. He, F. Ning, B. Li , Q. S. Song, W. Lv, H. Du, D. Zhai , F. Su, Q. H. Yang and F. Kang, *Journal of Power Sources*, 2012, **202**, 253-261.

29. L. Shen, C. Yuan, H. Luo, X. Zhang, S. Yang and X. Lu, *Nanoscale*, 2011, **3**, 572-574.

30. G.-N. Zhu, H.-J. Liu, J.-H. Zhuang, C.-X. Wang, Y.-G. Wang and Y.-Y. Xia, *Energy Environ. Sci.*, 2011, **4**, 4016-4022.

31. G.-Y. Liu, H.-Y. Wang, G.-Q. Liu, Z.-Z. Yang, B. Jin and Q.-C. Jiang, *Journal of Power Sources*, 2012, **220**, 84-88.

TOC

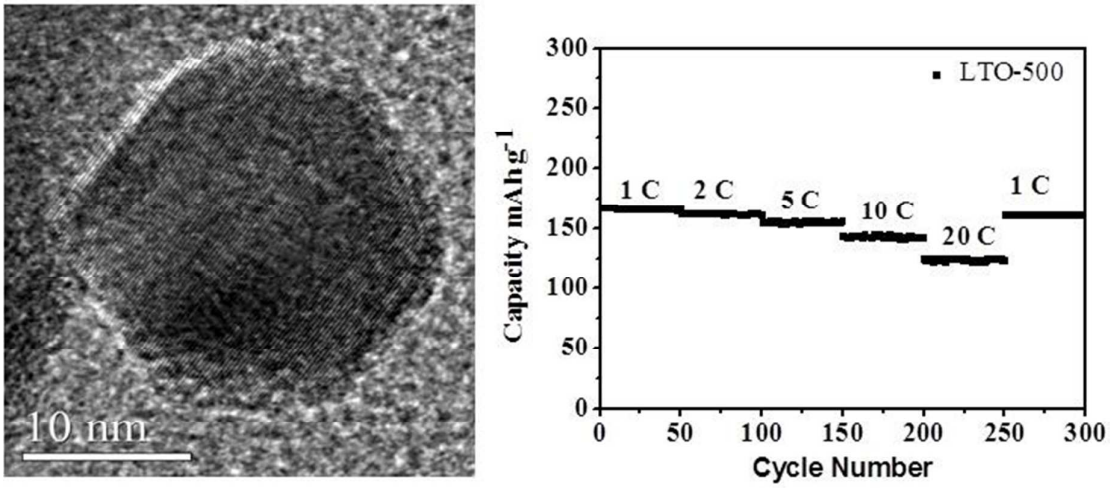

This is the first report about the preparation of highly crystallized $Li_4Ti_5O_{12}$ with a small particle size of ~20 under low synthesis temperature (500 ^oC).

Figure captions:

Fig.1 The TG-DSC curves of precursor

Fig.2 The XRD patterns of LTO calcined at different temperature

Fig. 3 TEM and HRTEM images of the LTO-400(a,b), LTO-500 (c,d) and LTO-600 (e,f)

Fig. 4 the cycle perofomance of LTO-400, LTO-500 and LTO-600

Fig. 5 the discharge curves of the LTO-400, LTO-500 and LTO-600 electrode

Fig 6.Electrochemical impedance spectra of pure LTO-500 and LTO-600 nanocomposites electrodes at the voltage of 1.55 V

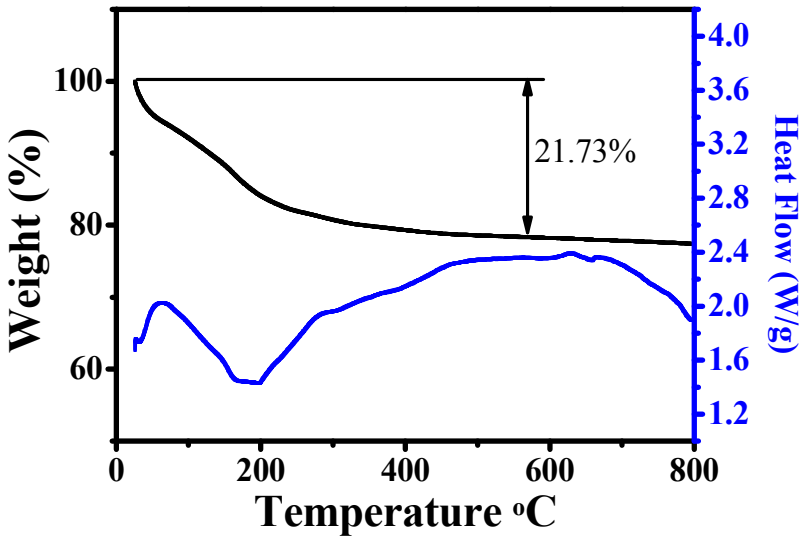

Fig.1 The TG-DSC curves of precursor

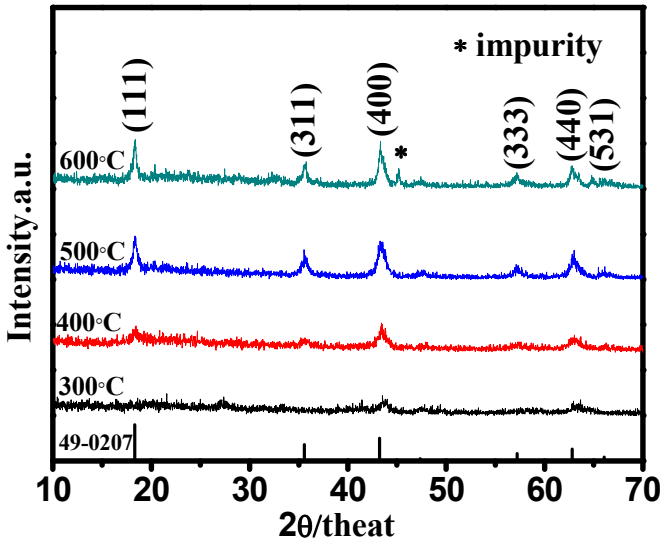

Fig.2 The XRD patterns of LTO calcined at different temperature

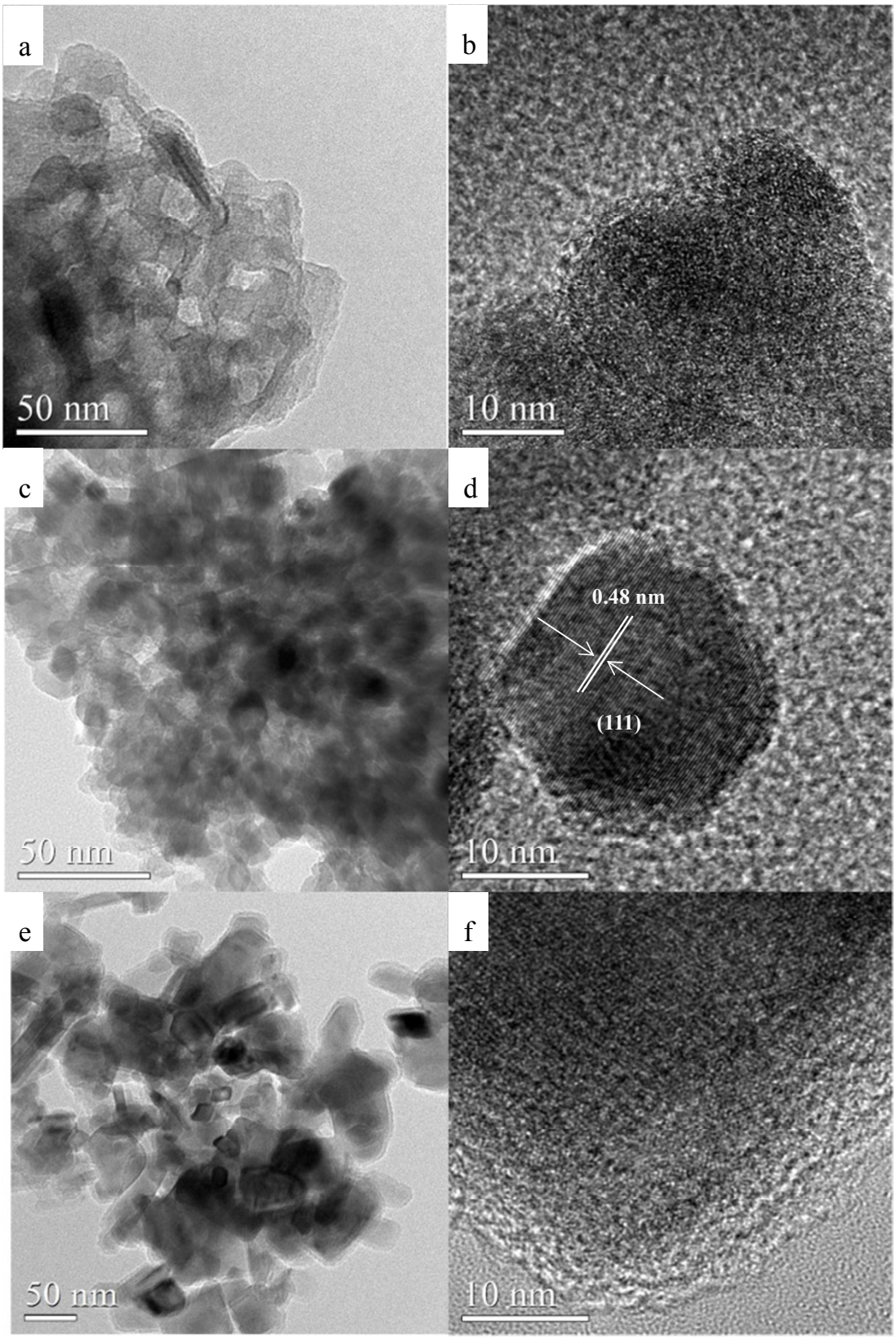

Fig. 3 TEM and HRTEM images of the LTO-400(a,b), LTO-500 (c,d) and LTO-600 (e,f)

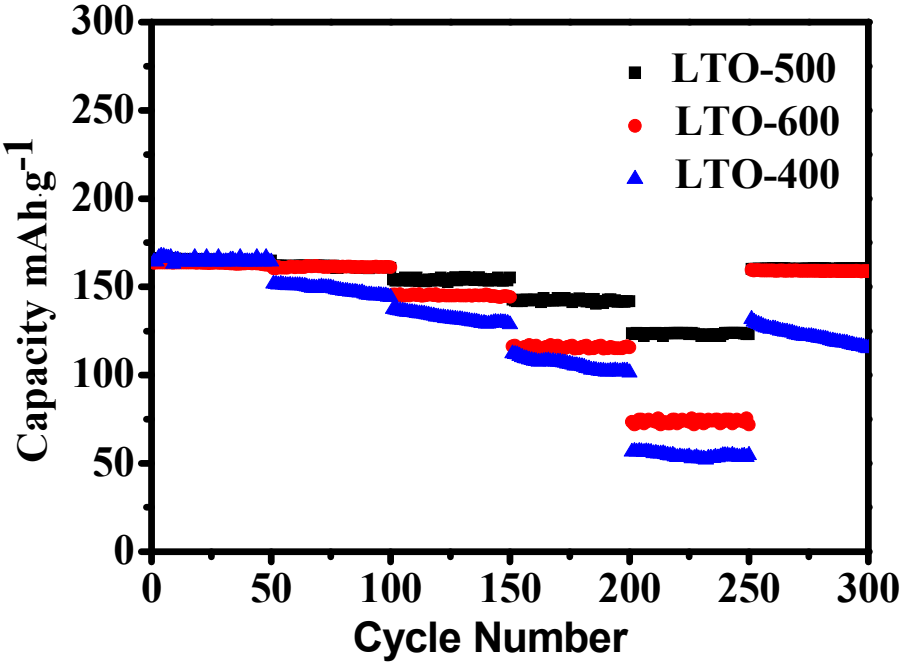

Fig. 4 the cycle perofomance of LTO-400,LTO-500 and LTO-600

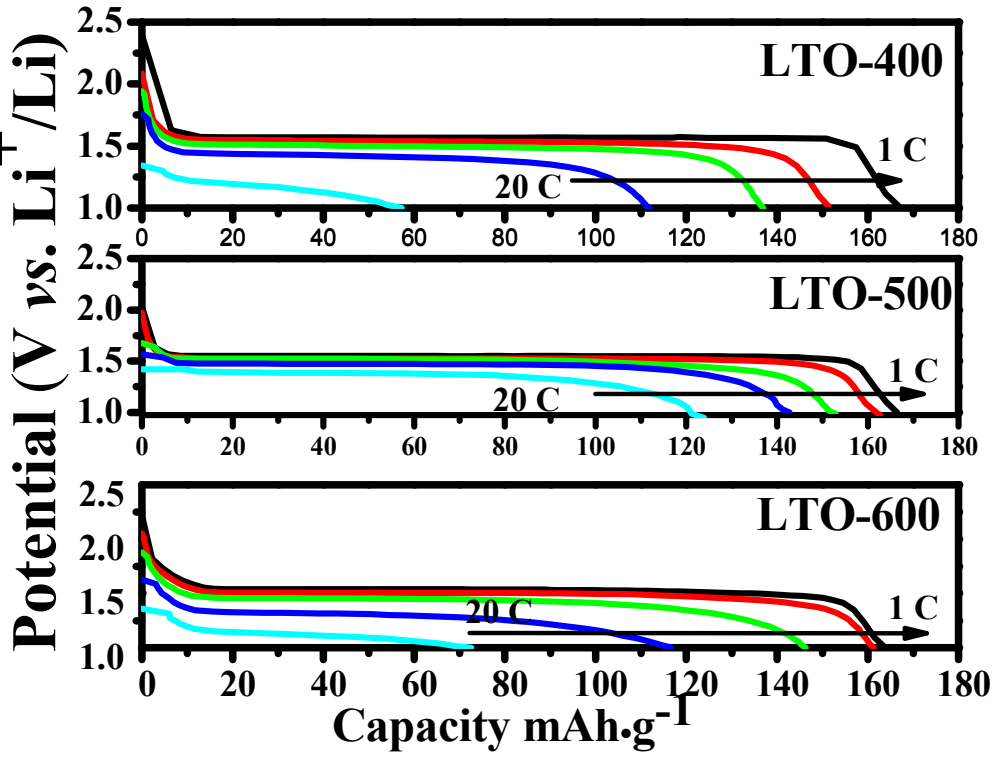

Fig 5. The discharge curves of the LTO-400, LTO-500 and LTO-600 electrode

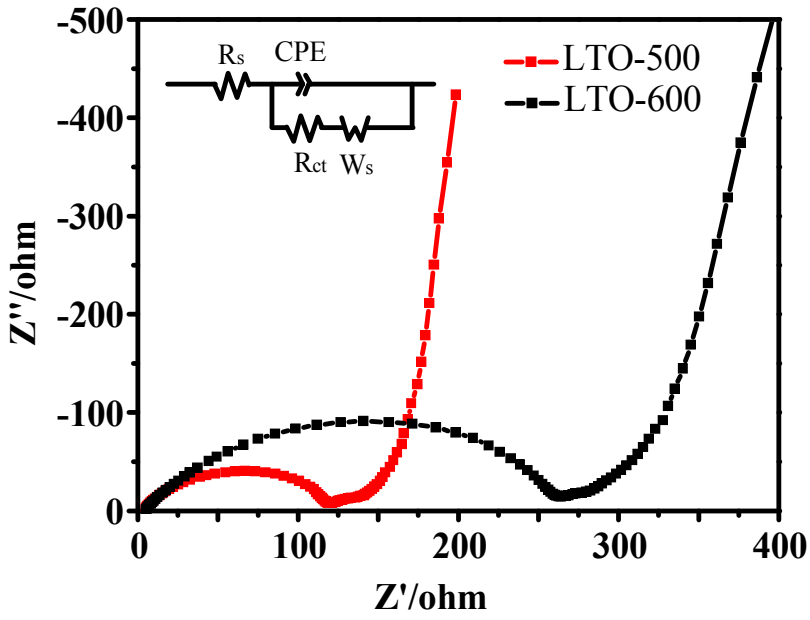

Fig 6.Electrochemical impedance spectra of pure LTO-500 and LTO-600 nanocomposites electrodes at the voltage of 1.55 V